On Obtaining Reactive Potential Energy Surfaces from Transition State Photodetachment Spectra. II. Inversion of Spectra in Model Systems

Ward H. Thompson†

Department of Chemistry, University of California, Berkeley, California 94720, and Department of Chemistry and Biochemistry, University of Colorado, Boulder, Colorado 80309-0215

Received: June 17, 1999; In Final Form: October 1, 1999

We present a method for determining reactive potential energy surfaces from experimental photodetachment spectra. The variations of the theoretical photodetachment spectrum with respect to potential parameters (the "derivatives" of the spectrum) are calculated. These derivatives are used in an iterative Levenberg−Marquardt-based algorithm to find the optimal values of the potential parameters, i.e., those yielding the theoretical spectrum that best matches the experimental one. Applications of the method to one- and two-degrees-of-freedom model systems are presented, and accurate results are obtained with a small number of iterations. Prospects for treating realistic systems are discussed.

1. Introduction

In the preceding paper[1] in this issue (hereafter referred to as Paper I) we carried out a sensitivity analysis of transition state (photodetachment) spectra. Specifically, for two model systems, we determined the regions of the neutral potential energy surface to which the spectra are sensitive. One of the primary conclusions drawn from that analysis is that the spectra are sensitive to the barrier region in a wide number of cases, including those where the Franck−Condon region (i.e., the location of the anion bound state) does not coincide with the transition state. This result suggests that it should be possible to use transition state spectra to obtain information about the barrier on the neutral potential surface. In this paper we present an iterative method for "inverting" a transition state spectrum to obtain an accurate representation of the neutral surface in the barrier region.

2. Methodology

In Paper I, we showed how the derivative of a photodetachment spectrum with respect to a parameter of the neutral potential energy surface can be obtained for no extra cost beyond that required to calculate the spectrum itself. In this section, we review the relevant formulas for completeness and then describe the methodology for "inverting" transition state spectra.

As in Paper I, we consider a potential surface for a chemical reaction defined by a set of M parameters $\boldsymbol{\alpha} = \{\alpha_j\}_{j=1,...,M}$. For the purposes of this paper the set $\boldsymbol{\alpha}$ will represent the parameters in an analytical representation of the potential energy surface. The derivative $\partial I(E)/\partial\alpha_j$ can be used to optimize the values of the potential parameters for which $\partial I(E)/\partial\alpha_j \neq 0$. Specifically, given an experimentally measured spectrum, $I_{ex}(E)$, at a set of N_E energies $\{E_i\}$ we can define a measure of the "error" in the trial spectrum as

$$\chi^2 = \sum_{i=1}^{N_E} [I(E_i; \boldsymbol{\alpha}) - I_{ex}(E_i)]^2 \tag{1}$$

The optimum potential is then the one that minimizes χ^2. Thederivative of χ^2 with respect to a potential parameter α_j indicates how the error changes as α_j is varied and is then given by

$$\frac{\partial\chi^2}{\partial\alpha_j} = 2\sum_{i=1}^{N_E} \frac{\partial I(E_i; \boldsymbol{\alpha})}{\partial\alpha_j} [I(E_i; \boldsymbol{\alpha}) - I_{ex}(E_i)] \tag{2}$$

Thus, the key to this approach is the calculation of the derivatives $\partial I(E)/\partial\alpha_j$.

In Paper I, we showed how these derivatives can be obtained using a Green's function in a discrete variable representation[2−4] (DVR) with absorbing boundary conditions[5−9] (ABC). This approach allows the calculation of the derivatives with no additional effort beyond that required to calculate the spectrum itself. Briefly, the photodetachment intensity in the DVR-ABC formulation is given within the Franck−Condon approximation by[10,11]

$$I(E) = -\frac{1}{\pi} Im\, \phi_b^T \cdot \Phi_b^+(E) \tag{3}$$

And, as shown in Paper I, the derivative of the intensity at energy E with respect to a potential parameter α_j is

$$\frac{\partial I(E)}{\partial\alpha_j} = -\frac{1}{\pi} Im\, \Phi_b^{+T}(E) \cdot \frac{\partial \mathbf{V}}{\partial\alpha_j} \cdot \Phi_b^+(E) \tag{4}$$

The scattering wavefunction $\Phi_b^+(E)$ is defined as

$$\Phi_b^+(E) = \mathbf{G}^+(E) \cdot \phi_b \tag{5}$$

where ϕ_b is the anion bound state wavefunction vector in the DVR and $\mathbf{G}^+(E)$ is the DVR-ABC Green's function:[12]

$$\mathbf{G}^+(E) = (E\mathbf{I} - \mathbf{H} + i\boldsymbol{\epsilon})^{-1} \tag{6}$$

with outgoing wave boundary conditions. Here, $\mathbf{H}$ and $\boldsymbol{\epsilon}$ are the DVR matrices of the Hamiltonian and the absorbing potential.

As can be seen from eqs 3−5 the primary effort in calculating the photodetachment intensity, $I(E)$, and its derivative with respect to a potential parameter, $\partial I(E)/\partial\alpha_j$, is the same: the action of the Green's function onto the anion bound state. Thus,

† Current address. University of Colorado.

10.1021/jp992022h CCC: $18.00
Published on Web 10/27/1999

any and all derivatives of the spectrum can be obtained with no extra effort beyond that required to compute $I(E)$ itself. In addition, we note that, in principle, the entire photodetachment spectrum can be obtained in a single calculation using the quasi-minimal residual (QMRES) method[13] for acting the Green's function on the anion bound state.[11]

A generic iterative scheme for obtaining the neutral potential energy surface from an experimental photodetachment spectrum is as follows:

(1) Make an initial guess for the potential, $\tilde{V}$.

(2) Calculate the photodetachment spectrum (and its derivatives) associated with $\tilde{V}$ using eqs 3−5.

(3) Calculate the "error" of the theoretical spectrum relative to the experimental one using eq 1.

(4) Use the derivatives $\partial I(E)/\partial \alpha_j$ to obtain a new $\tilde{V}$.

(5) Return to 2, iterating until χ^2 is minimized.

A variety of schemes of this sort can be conceived, particularly several that differ only in the method used in Step 4. In this paper we use a Levenberg−Marquardt algorithm[14] for implementing this scheme. This algorithm uses a combination of the inverse-Hessian and steepest descent methods to update the parameters to be optimized, $\{\alpha_j\}_{j=1,...,M}$.

On the basis of sensitivity analysis in Paper I, it seems unlikely that, in general, an accurate "point-by-point" representation of the potential surface can be obtained by inverting transition state spectra. An extreme example is the case where the Franck−Condon region is in the reactant valley. If photodetachment of the anion does not lead to formation of the neutral products then the spectrum contains no information about the product side of the potential. Nevertheless, as seen in Paper I, the photodetachment spectrum can still provide information about the barrier region in this case. Thus, here we consider the optimization of parameters in an analytical representation of the neutral surface. The goal is to establish the viability and properties of the present approach by treating model systems. Thus, the "experimental" spectrum is generated by a theoretical calculation using one potential (what we will call the exact potential). Then the "experimental" spectrum is used to optimize the parameters of a trial potential with a different functional form by minimizing the error of the theoretical spectrum (obtained using the trial potential) relative to the "experimental" one.

3. Model Systems

A. One-Dimensional Barrier. As a first test of the method proposed in Section 2, we consider a one-dimensional model problem in which the exact (i.e., "experimental") spectra are those for the Eckart barrier model considered in Paper I.[1,15] The exact, or target, neutral potential is given by

$$V_{ex}(q) = V_0^{ex}\mathrm{sech}^2(q/a) \tag{7}$$

with $V_0^{ex} = 0.425$ eV and $a = 1$ au and the anion potential is a harmonic oscillator of frequency $\omega = 3000$ cm^{-1} centered at q_0. The mass is taken to be 1060 au and in what follows we consider both $q_0 = 0$ and $q_0 = 1$ au. The trial potential has a different functional form and is a Gaussian,

$$\tilde{V}(q) = V_0 e^{-bq^2} \tag{8}$$

where V_0 and b are the parameters to be optimized using the "experimental" spectrum.

The test of the method is as follows. The "experimental" photodetachment spectrum, $I_{ex}(E)$, is first calculated at 60 values of the scattering energy using the exact potential, eq 7. Initial guesses are made for the parameters V_0 and b in the trial potential. The Levenberg−Marquardt-based scheme described in Section 2 is then used to minimize the error χ^2 (eq 1) of the theoretical spectrum $I(E)$ obtained with the trial potential, eq 8, relative to $I_{ex}(E)$.

Figure 1a shows the initial, optimized, and "experimental" photodetachment spectra resulting from this exercise for the case where $q_0 = 0$ and initially $V_0 = 0.7$ eV and $b = 1.4$ au. Here the spectra are for photodetachment from the anion ground state ($\upsilon = 0$). The initial trial potential gives a spectrum peaking at significantly higher energy than the exact spectrum due to the greater barrier height. However, the spectrum obtained from the optimized trial potential is in excellent agreement with the exact spectrum. Figure 2a shows the error χ^2 (on a semilog plot) and the values of V_0 and b at each iteration of the optimization. Convergence is achieved in 15 iterations yielding excellent agreement in the barrier height with optimized values of $V_0 = 0.424$ eV and $b = 0.977$ au. Note that while there is a plateau in the value of χ^2 it decreases monotonically with the number of iterations. It is interesting that the value of b initially increases by an order of magnitude from its initial value before converging to its optimum value. On the other hand, the route of the barrier height to its final value is much more direct.

Figure 1b shows the initial, optimized, and "experimental" photodetachment spectra from the $\upsilon = 1$ anion state with $q_0 = 0$. The initial parameters in the trial potential are taken as $V_0 = 1.0$ eV and $b = 0.6$ au. These result in a spectrum peaked at very high energies (in fact the intensity is nonzero outside the range of energies considered in the optimization). Despite the initial barrier height being more than twice the exact value, the optimization is completed in 16 iterations giving a spectrum in excellent agreement with the "experimental" one.

The error in the theoretical spectrum and the values of the trial potential parameters are shown in Figure 2b as a function of the number of iterations. As in Figure 2a, χ^2 decreases monotonically while b initially increases by an order of magnitude before converging (to 0.948 au). Here the value of V_0 first increases to ~1.4 eV before decreasing to its optimized value of 0.422 eV, in excellent agreement with the barrier height of the exact potential.

The initial, optimized, and "experimental" photodetachment spectra from the anion ground state with $q_0 = 1$ au are shown in Figure 1c. The initial values of V_0 and b are taken to be 0.2 eV and 0.6 au, respectively. The initial spectrum is quite different from the "experimental" one; it is peaked at a significantly lower energy and consists of a narrow peak with a shoulder at higher energy whereas the exact spectrum consists of two distinct broad peaks with the second having much less intensity. The optimized spectrum is in excellent agreement with the exact spectrum reproducing both the position and width of the peaks.

The convergence of the error in the theoretical spectrum and the trial potential parameters is shown for this case in Figure 2c. The behavior observed here is notably different from that in Figure 2, parts a and b. First, convergence is achieved in significantly fewer iterations, 9 vs ~15. Second, both V_0 and b rise almost monotonically to their optimized values of 0.404 eV and 0.81 au, respectively. As before, χ^2 decreases monotonically. The final barrier height is slightly lower than that obtained in the previous cases with $q_0 = 0$, but is still in excellent agreement within 0.5 kcal/mol of the exact value.

Note that the different choices for the anion bound state used to obtain the spectrum (i.e., the values of υ and q_0) do not lead

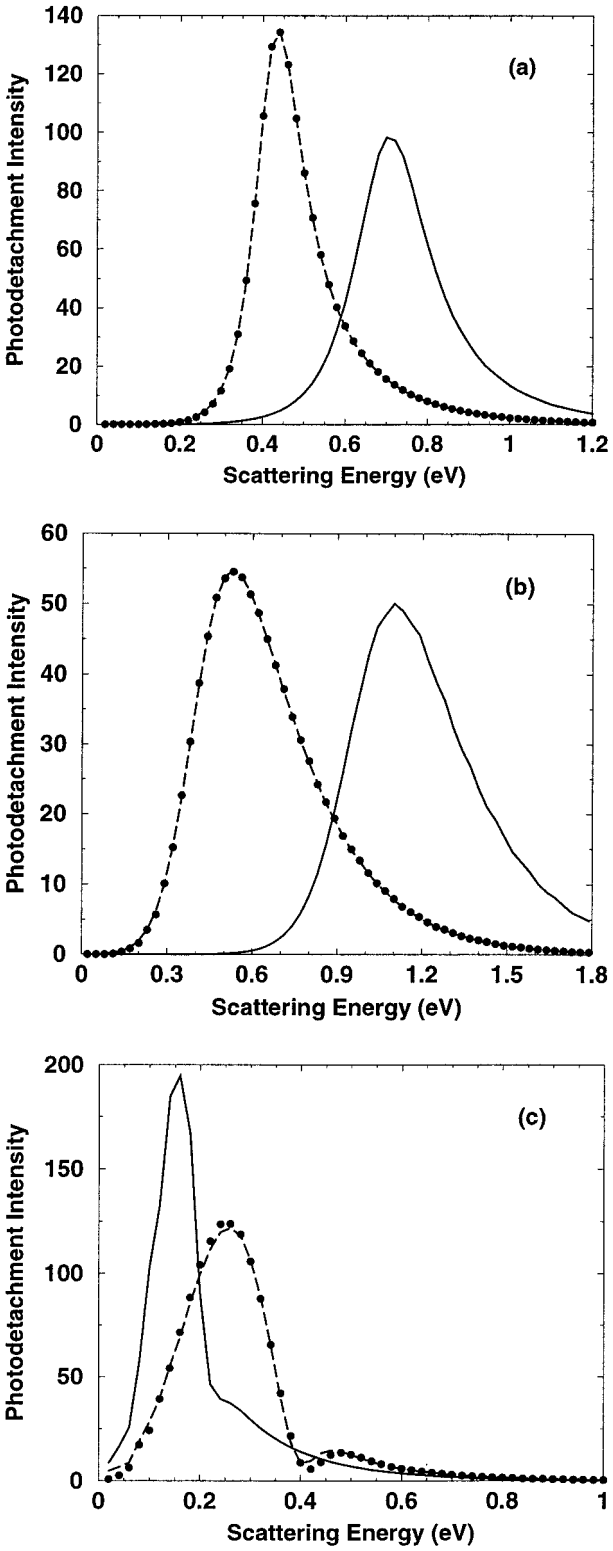

Figure 1. The initial, optimized, and "experimental" photodetachment spectra for the one-dimensional model are plotted. In each case, the initial spectrum is shown as the solid line, the optimized spectrum as the dashed line, and the "experimental" spectrum ($V_0 = 0.425$ eV, $a =$ 1.0 au) as the solid circles. Results are shown for photodetachment from (a) the $v = 0$ anion state with $q_0 = 0$, (b) the $v = 1$ anion state with $q_0 = 0$, and (c) the $v = 0$ anion state with $q_0 = 1$ au. The initial and optimized potential parameters are given in the text.

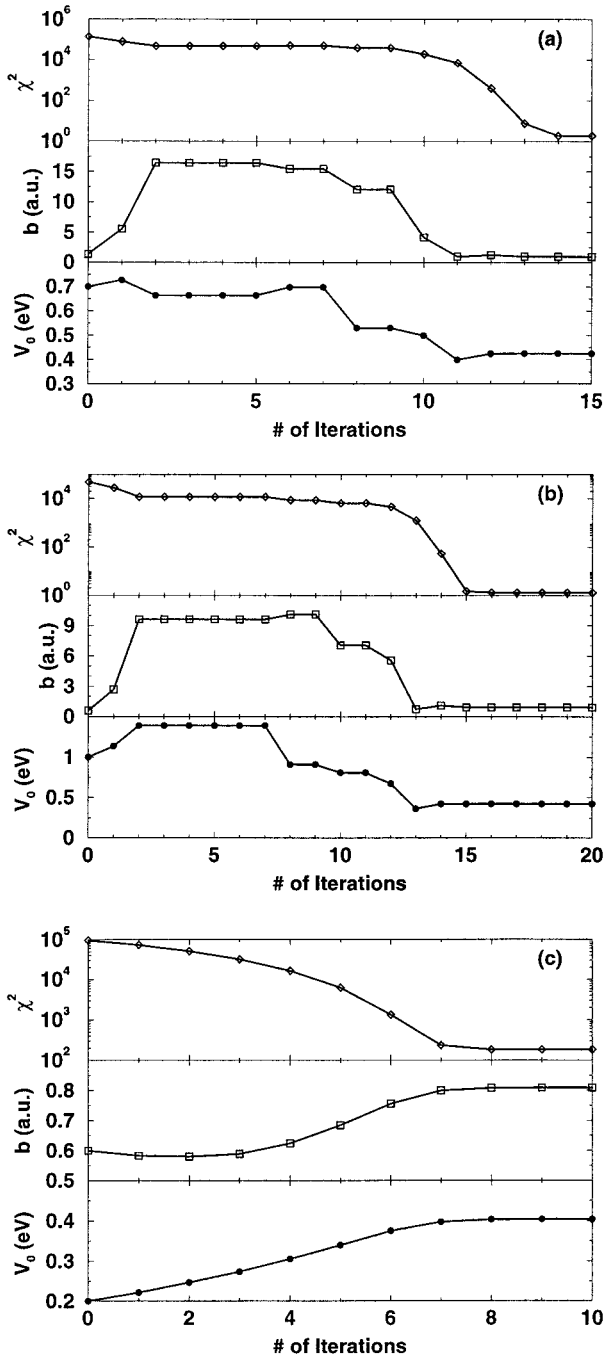

Figure 2. The error χ^2 and potential parameters V_0 and b for the optimization of the potential, corresponding to the cases shown in Figures 1a−c, are plotted as a function of the number of iterations in the optimization. Again, results are shown for photodetachment from (a) the $v = 0$ anion state with $q_0 = 0$, (b) the $v = 1$ anion state with $q_0 = 0$, and (c) the $v = 0$ anion state with $q_0 = 1$ au.

to the same optimized V_0 and b. This is a consequence of using a different functional form for the exact and trial potentials. Each anion state probes somewhat different regions of the neutral potential and the optimized values of the trial potential parameters are those that best match the trial and exact potentials in those regions. Note that in all cases the optimized photodetachment spectra are in excellent agreement with the "experimental" spectra. However, we saw that for $q_0 = 0$ the $v = 0$ and $v = 1$ anion states yield slightly different optimized values of V_0 and b. And, for the $v = 0$, $q_0 = 1$ au anion state we obtained an optimum value of b that is ∼15% lower and a slightly lower value for V_0. The initial, optimized, and exact neutral potentials for this case are shown in Figure 3. Note that the optimum potential is indistinguishable from the exact potential on the sides of the barrier. Also, while the final barrier

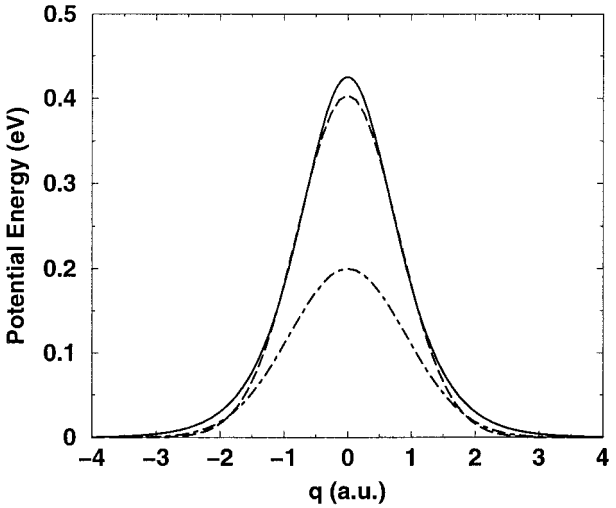

Figure 3. The initial, optimized, and exact potentials for the one-dimensional model problem are plotted. The results shown are from the optimization carried out using the photodetachment spectrum from the $v = 0$ anion state with $q_0 = 1$ au. The exact (Eckart barrier) potential is shown as the solid line while the initial and optimized (Gaussian) potentials are indicated by the dot−dashed and dashed lines, respectively.

height is somewhat low, it is still in excellent agreement with the exact value.

B. Collinear H + H_2. As a second example we consider a two-degrees-of-freedom model system in which the neutral potential energy surface is that for the collinear H + H_2 reaction. In this case, the exact neutral potential is given by the LSTH surface[16] which has a barrier height of 0.425 eV.[1,17] The "experimental" photodetachment spectrum is obtained using this potential with a separable harmonic oscillator anion potential in the Jacobi coordinates of the reactant arrangement,

$$v_{\text{anion}}(r, R) = \frac{1}{2}\mu_r\omega_r^2(r - r_0)^2 + \frac{1}{2}\mu_R\omega_R^2(R - R_0)^2 \quad (9)$$

Here r and R are the vibrational and translational Jacobi coordinates, respectively, with associated reduced masses μ_r and μ_R. As in Paper I, we consider two sets of parameters for the anion potential with $\omega_r = 2500$ cm^{-1} and $\omega_R = 2000$ cm^{-1} in both cases. Set A has an equilibrium geometry identical to that of the neutral transition state with $r_0 = 1.757$ au and $R_0 = 2.6355$ au. For Set B the equilibrium geometry is displaced into the reactant valley with $r_0 = 1.6$ au and $R_0 = 3.2$ au.

The trial potential to be optimized is of the London−Eyring−Polanyi−Sato (LEPS) form,

$$\tilde{V}(r, R) = Q_{\text{ab}} + Q_{\text{ac}} + Q_{\text{bc}} - \sqrt{J_{\text{ab}}^2 + J_{\text{ac}}^2 + J_{\text{bc}}^2 - J_{\text{ab}}J_{\text{ac}} - J_{\text{ab}}J_{\text{bc}} - J_{\text{ac}}J_{\text{bc}}} \quad (10)$$

where a, b, and c label the three atoms and, e.g.,

$$Q_{\text{ab}} = \frac{1}{4}D[(3 + S^2)e^{-2\beta(r_{\text{ab}} - r_0)} - (2 + 6S^2)e^{-\beta(r_{\text{ab}} - r_0)}]/(1 + S^2) \quad (11)$$

and

$$J_{\text{ab}} = \frac{1}{4}D[(1 + 3S^2)e^{-2\beta(r_{\text{ab}} - r_0)} - (6 + 2S^2)e^{-\beta(r_{\text{ab}} - r_0)}]/(1 + S^2) \quad (12)$$

Here D, β, and r_0 are the Morse parameters for the diatomic fragment; by symmetry these parameters are the same for each pair and can be obtained from the well-known diatomic H_2 potential. The values are taken to be $D = 4.75$ eV, $\beta = 1.044$ au, and $r_0 = 1.42$ au. The Sato parameter, S, is here the parameter to be optimized by minimizing the error of the theoretical photodetachment spectrum relative to the "experimental" one.

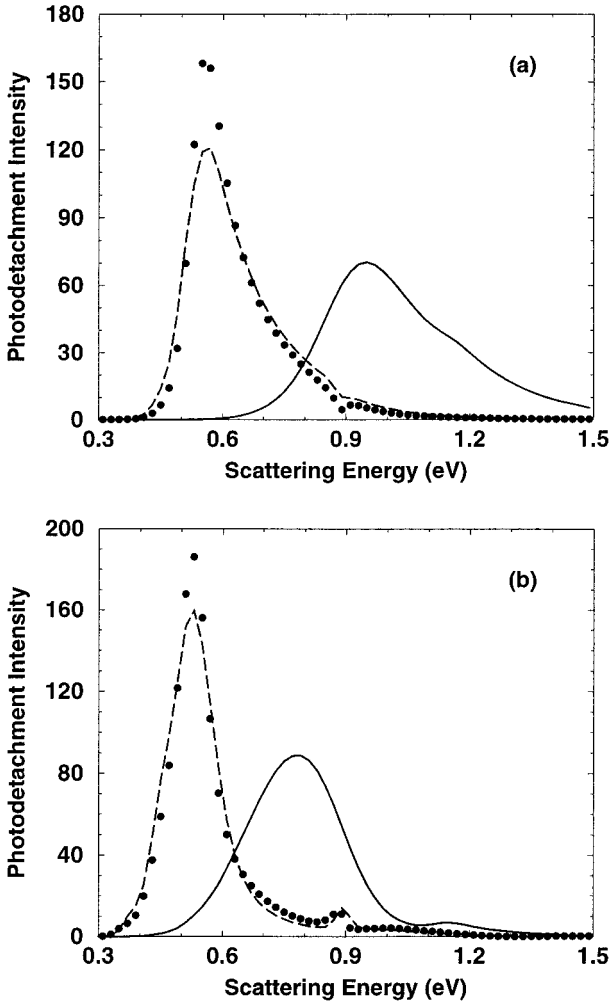

Figure 4. The "experimental", initial, and optimized photodetachment spectra for the collinear H_3^- model are plotted. Results using the anion potential parameter (a) Set A and (b) Set B are shown. The initial spectra ($S = 0.2$ corresponding to $V_0 = 0.828$ eV) are plotted as solid lines, the optimized spectrum ($S = 0.355$ corresponding to $V_0 = 0.439$ eV for Set A and $S = 0.347$ corresponding to $V_0 = 0.464$ eV for Set B) as dashed lines, and the "experimental" spectra ($V_0 = 0.425$ eV) as the solid circles.

For parameter Set A, Figure 4a shows the "experimental" spectrum calculated using the LSTH potential and the initial and optimized spectra from the LEPS surface. The initial value of S is taken as 0.2 corresponding to a barrier height of 0.828 eV. Due to the larger barrier height the initial spectrum is shifted to higher energy and broadened relative to the exact one. The optimized spectrum obtained after 15 iterations is in very good agreement with the "experimental" one, the primary difference being that the peak maximum has a lower value. Note that the sharp dip at ~0.9 eV due to the production of H_2 ($v = 1$)[1] is well reproduced. Plots of the analogous photodetachment spectra for parameter Set B are shown in Figure 4b for the same initial S. The results are much the same for this displaced anion geometry as observed for Set A. The initial spectrum peaks at a higher energy and is broadened while the optimized spectrum

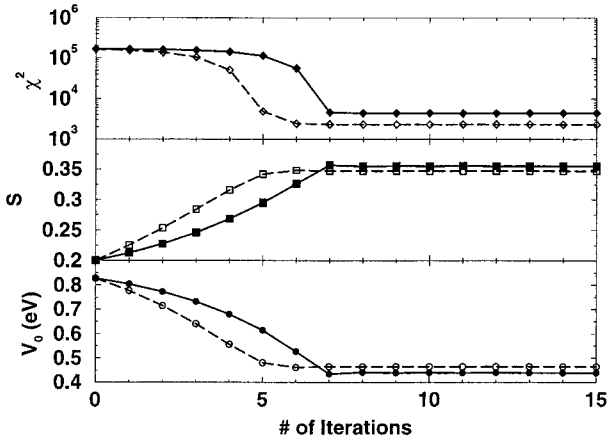

Figure 5. The error χ^2, Sato parameter S, and corresponding barrier height V_0 for the optimizations of the LEPS potential corresponding to Figure 4 are plotted as a function of the number of iterations. The results are shown for anion potential parameter Set A as the solid lines with filled symbols and for Set B as the dashed lines with open symbols.

is in quite good agreement with a minor difference in the peak maximum. This is true even though the anion bound state wave function for Set B has little overlap with the barrier region of the neutral potential.

Figure 5 shows the error in the theoretical spectrum, χ^2, the value of the Sato parameter, and the corresponding barrier height at each iteration for both the Set A and Set B cases. As seen for the one-dimensional example above, the different anion states lead to slightly different values of the optimized parameter. Using Set A the optimum value of S is found to be 0.355 while Set B yields 0.347. This difference naturally leads to different barrier heights in the optimized potentials, giving values of 0.439 and 0.464 eV for Sets A and B, respectively. It is worth noting that these are within <1 kcal/mol of the exact barrier height. In both cases the convergence of the Sato parameter is smooth and rapid, being completed in 10 iterations.

One factor that can limit the effectiveness of an inversion procedure is finite experimental resolution. This can be reasonably represented by Gaussian convolution of the theoretical spectrum. That is, in making a comparison with an experimental spectrum the theoretical spectrum to be used is given by

$$I_c(E) = N \int I(E')\, e^{-(E-E')^2/\eta^2}\, dE' \qquad (13)$$

where N is a normalization constant determined, e.g., by scaling to match the maximum value of the experimental spectrum. We can examine the effect on the inversion of the transition state spectra by generating an "experimental" spectrum by convoluting the calculated spectrum for the exact potential.

To this end, we have optimized the LEPS potential using the H_3^- spectrum calculated using the LSTH potential (with anion potential parameter Set B) and convoluted with $\eta = 0.01$ eV, a reasonable experimental value. Since the exact resolution may not always be known, we convolute the trial spectra with a different value, $\tilde{\eta} = 0.008$ eV. The initial, optimized, and exact (convoluted) spectra are shown in Figure 6 for this case. Note that the optimized spectrum is in very good agreement with the "experimental" spectrum. The optimized value of the Sato parameter is 0.347, corresponding to a barrier height of 0.466 eV. The convergence is smooth, similar to that in Figure 5, and is completed in 15 iterations. Thus, excellent agreement with the exact barrier height is obtained despite the convolution and the use of different values of η for the exact and trial spectra.

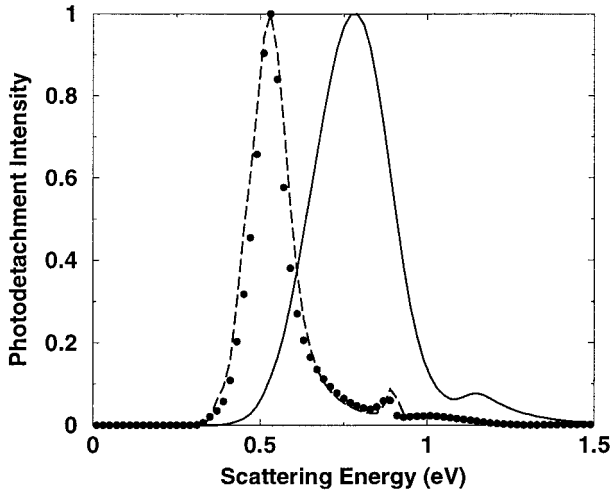

Figure 6. Same as Figure 4b but the "experimental" spectrum has been convoluted with $\eta = 0.01$ eV (cf. eq 13) and the trial spectra with $\tilde{\eta} = 0.008$ eV (see the text). Here the optimized spectrum has $S = 0.347$ corresponding to $V_0 = 0.466$ eV.

In fact, while a somewhat larger number of iterations is required, the final values of the Sato parameter is almost identical (within 0.001) to the unconvoluted case.

4. Concluding Remarks

We have presented a method for determining reactive potential energy surfaces from transition state photodetachment spectra. The method makes use of the derivatives of the photodetachment spectra with respect to parameters of the neutral potential energy surface. As shown previously,[1] these derivatives can be obtained at no additional cost above that required to calculate the spectrum itself. An iterative Levenberg−Marquardt-based scheme is used to optimize the potential parameters by minimizing the differences between the theoretical and experimental photodetachment spectra.

The viability of this approach has been demonstrated by its application to two model systems. Excellent agreement is obtained with the barrier height on the neutral potential energy surfaces in all cases. The method converges rapidly and thus requires only a small number of calculations of the photodetachment spectrum (and its derivatives). In addition, the finite resolution of experimental spectra can be dealt with by convolution of the theoretical spectrum and does not hinder the determination of the potential surface even if the resolution is not known exactly.

It is worth noting that multiple spectra for the same system obtained with different initial anion bound states can be used to advantage in this method. The measure of the error in eq 1 (which is minimized) can be simply extended to include more than one spectrum. The development of experimental techniques for varying the anion wave function would thus improve the ability to accurately determine the neutral potential surface.

There are a number of systems that would be interesting to treat with this method. These include the XHY^- systems (the X + HY reactions), where X and Y are halides. The photodetachment spectra of these anions have been the subject of extensive experimental studies.[18] In addition, larger molecules are such as cyclooctatetraene[19] are of interest which, while not amenable to a full-dimensional quantum mechanical description, can be accurately treated in reduced dimensionality. In the case of cyclooctatetraene the photodetachment spectrum probes the barrier to isomerization of the molecule.

Acknowledgment. I gratefully acknowledge Prof. William H. Miller for his support and encouragement as wells as for productive conversations, and Prof. James T. Hynes for his support during the completion of this work. I also thank Profs. Daniel M. Neumark and W. Carl Lineberger for useful discussions.

References and Notes

(1) Thompson, W. H. *J. Phys. Chem. A* **1999**, *103*, 9500.

(2) Dickinson, A. S.; Certain, P. R. *J. Chem. Phys.* **1963**, *49*, 4209; Harris, D. O.; Engerholm, G. G.; Gwinn, W. D. *J. Chem. Phys.* **1965**, *43*, 1515.

(3) Lill, J. V.; Parker, G. A.; Light, J. C. *Chem. Phys. Lett.* **1982**, *89*, 483; Light, J. C.; Hamilton, I. P.; Lill, J. V. *J. Chem. Phys.* **1985**, *82*, 1400; Bačić, Z.; Light, J. C. *J. Chem. Phys.* **1986**, *85*, 4594; Whitnell, R. M.; Light, J. C. *J. Chem. Phys.* **1988**, *89*, 3674; Choi, S. E.; Light, J. C. *J. Chem. Phys.* **1990**, *92*, 2129.

(4) Colbert, D. T.; Miller, W. H. *J. Chem. Phys.* **1992**, *96*, 1982.

(5) Goldberg, A.; Shore, B. W. *J. Phys. B* **1978**, *11*, 3339.

(6) Leforestier, C.; Wyatt, R. E. *J. Chem. Phys.* **1983**, *78*, 2334.

(7) Jolicard, G.; Austin, E. J. *Chem. Phys. Lett.* **1985**, *121*, 106; Jolicard, G.; Austin, E. J. *Chem. Phys.* **1986**, *103*, 295; Jolicard, G.; Perrin, M. Y. *Chem. Phys.* **1987**, *116*, 1; Jolicard, G.; Leforestier, C.; Austin, E. J. *J. Chem. Phys.* **1988**, *88*, 1026.

(8) Kosloff, R.; Kosloff, D. *J. Comput. Phys.* **1986**, *63*, 363.

(9) Neuhauser, D.; Baer, M. *J. Chem. Phys.* **1989**, *90*, 4351; Neuhauser, D.; Baer, M. *J. Chem. Phys.* **1989**, *91*, 4651; Neuhauser, D.; Baer, M.; Kouri, D. J. *J. Chem. Phys.* **1990**, *93*, 2499.

(10) Thompson, W. H.; Miller, W. H. *J. Chem. Phys.* **1994**, *101*, 8620.

(11) Thompson, W. H.; Karlsson, H. O.; Miller, W. H. *J. Chem. Phys.* **1996**, *105*, 5387.

(12) Seideman, T.; Miller, W. H. *J. Chem. Phys.* **1992**, *96*, 4412; Seideman, T.; Miller, W. H. *J. Chem. Phys.* **1992**, *97*, 2499; Miller, W. H.; Seideman, T. In *Time Dependent Quantum Molecular Dynamics: Experiment and Theory*; Broeckhove, J., Ed.; NATO ARW 1992; Thompson, W. H.; Miller, W. H. *Chem. Phys. Lett.* **1993**, *206*, 123.

(13) Freund, R. W.; Nachtigal, N. M. *Numer. Math.* **1991**, *60*, 315; Freund, R. W. In *Numerical Linear Algebra*; Reichel, L., Ruttan, A., Varga, R., Eds.; de Gruyter: Berlin, 1993.

(14) Press, W. H.; Flannery, B. P.; Teukolsky, S. A.; Vetterling, W. T. *Numerical Recipes, The Art of Scientific Computing*; Cambridge University Press: Cambridge, UK, 1992.

(15) Thompson, W. H. Ph.D. Thesis, Lawrence Berkeley Laboratory, University of California, 1996.

(16) Liu, B.; Siegbahn, P. *J. Chem. Phys.* **1978**, *68*, 2457; Truhlar, D. G.; Horowitz, C. *J. Chem. Phys.* **1978**, *68*, 2566; *J. Chem. Phys.* **1979**, *71*, 1514.

(17) Spath, B. W.; Miller, W. H. *Chem. Phys. Lett.* **1996**, *262*, 486.

(18) See, for example, Neumark, D. M. *Acc. Chem. Res.* **1993**, *26*, 33; Metz, R. B.; Bradforth, S. E.; Neumark, D. M. *Adv. Chem. Phys.* **1992**, *81*, 1; Bradforth, S. E.; Weaver, A.; Arnold, D. W.; Metz, R. B.; Neumark, D. M. *J. Chem. Phys.* **1990**, *92*, 7205; Waller, I. M.; Kitsopoulos, T. N.; Neumark, D. M. *J. Phys. Chem.* **1990**, *94*, 2240; Metz, R. B.; Weaver, A.; Bradforth, S. E.; Kitsopoulos, T. N.; Neumark, D. M. *J. Phys. Chem.* **1990**, *94*, 1377; Weaver, A.; Metz, R. B.; Bradforth, S. E.; Neumark, D. M. *J. Phys. Chem.* **1988**, *92*, 5558; Metz, R. B.; Kitsopoulos, T.; Weaver, A.; Neumark, D. M. *J. Chem. Phys.* **1988**, *88*, 1463.

(19) Wenthold, P. G.; Hrovat, D. A.; Borden, W. T.; Lineberger, W. C. *Science* **1996**, *272*, 1456.